



Article

Biomechanical Evaluation of PEEK and PLA Composite Femoral Implants for Stress Shielding Reduction: A Finite Element Simulation Study

Dario Milone *  and Marta Spataro 

Department of Engineering, University of Messina, Contrada di Dio, 98166 Messina, Italy;
marta.spataro@studenti.unime.it

* Correspondence: dmilone@unime.it

Featured Application: The findings of this study suggest that composite materials like PEEK and PLA, especially when reinforced with hydroxyapatite, may offer advantages over traditional titanium in reducing stress shielding and promoting a more favorable load distribution at the bone–implant interface. Their mechanical compatibility with bone could support better bone preservation and potentially contribute to longer implant lifespans.

Abstract: Background: Total hip arthroplasty (THA) is a widely adopted surgical intervention for restoring mobility and reducing pain in patients with severe hip joint conditions, such as osteoporosis. However, traditional titanium implants often lead to stress shielding and subsequent bone resorption due to the mismatch in stiffness between the implant and bone. Objectives: This study computationally investigates the biomechanical performance of femoral implants made from composite materials, specifically polyether-ether-ketone (PEEK) and polylactic acid (PLA) reinforced with hydroxyapatite (HA), compared to conventional titanium stems. Methods: Using finite element (FE) modeling, physiological loading during walking was simulated, and the strain energy density (SED) was analyzed to assess stress distribution and the potential for stress shielding across different Gruen zones. Results: The results indicate that both the PEEK and PLA composites exhibited more physiological load transfer, particularly in Gruen zones 1 and 7, reducing stress shielding and supporting bone preservation. Conclusions: These findings suggest that PEEK and PLA composites may offer improved implant stability and bone integration. Despite highlighting the promise of biomimetic materials in orthopedics, this study is limited to computational analysis and requires experimental validation. It emphasizes the need for further investigation using patient-specific geometries and a variety of loading scenarios to confirm these benefits and optimize femoral implant design.

Keywords: total hip arthroplasty (THA); femoral implants; biomechanical performance; bone preservation; implant stability; biomimetic materials



Academic Editor: Giuseppe Solarino

Received: 10 March 2025

Revised: 17 April 2025

Accepted: 18 April 2025

Published: 23 April 2025

Citation: Milone, D.; Spataro, M. Biomechanical Evaluation of PEEK and PLA Composite Femoral Implants for Stress Shielding Reduction: A Finite Element Simulation Study. *Prosthesis* **2025**, *7*, 44. <https://doi.org/10.3390/prosthesis7030044>

Copyright: © 2025 by the authors. Licensee MDPI, Basel, Switzerland.

This article is an open access article distributed under the terms and conditions of the Creative Commons Attribution (CC BY) license (<https://creativecommons.org/licenses/by/4.0/>).

1. Introduction

The hip joint is a crucial weight-bearing joint, making it vulnerable to musculoskeletal conditions like osteoporosis. In Europe, the prevalence of osteoporosis is projected to rise significantly, increasing by approximately 1.06 million cases, from 4.28 million in 2019 to an estimated 5.34 million by 2034 [1]. When such conditions severely impact joint function,

causing intense pain that greatly restricts movement, total hip arthroplasty (THA) is often performed as a treatment to restore mobility and alleviate pain [2–4].

Aside from the surgical technique and infections, the long-term success of cementless implants relies on bone growth onto the implant's surface joint replacements. To promote this, micromotions at the implant–bone interface must be minimized, as they can cause loosening, component failure, osteolysis, and stress shielding [3,5].

Over time, the design and performance of implants have improved considerably, with the aim to reduce failure and enhancing patients' quality of life [6–8]. Implant fixation relies on implant design and material, which help minimize gaps, reduce movement, and optimize host responses between the implant and host bone [9].

The most common materials for THA include titanium alloys such as Ti-6Al-4V, chosen for their light weight, resistance to corrosion, and biocompatibility [10].

However, bone adapts to the mechanical environment in which it is present, and the greater stiffness of metal implants compared with natural bone often results in bone resorption in areas that are not loaded [11]. To address this issue, previous research has focused on optimizing implant geometry, incorporating lattice structures, and exploring the use of novel materials to reduce bone loss in these regions [12].

In this context, finite element (FE) models are widely used to evaluate the potential impact of composition changes in stems on bone [13–19]. These models, alone or combined with experimental studies, serve as valuable preclinical tools for evaluating implant performance. Biomechanical analysis through FE simulations helps examine the post-operative mechanical environment of the implant–bone structure [20]. The reliability of this method for the clinical translation of these models is supported by experimental validation. A literature review conducted by van de Munckhof et al. demonstrated the potential of subject-specific FE models to predict fracture load with reasonable accuracy when compared with in vitro experiments, reporting R^2 values up to 0.96 and percentage errors generally within 10–20% [21]. Similarly, micro-FE models derived from high-resolution imaging have shown excellent reproducibility and predictive value for bone strength, particularly in distal sites like the radius and tibia [22]. Furthermore, Schileo et al. demonstrated that incorporating strain-based failure criteria into subject-specific models improves the identification of fracture onset locations, reinforcing the importance of experimental validation for refining FE methodologies [23].

Arabnejad et al. developed a fully porous hip implant with an internal tetrahedral structure designed to optimize density distribution across the implant. This innovative design significantly minimized bone loss from stress shielding, reducing it by approximately 75% compared with a traditional solid, non-porous implant [24]. Cortis et al. designed a porous hip stem using a body-centered-cube unit cell structure made from Ti6Al4V alloy. This design led to a reduction in stress shielding by 11% in Gruen zone 6 and 25% in zone 7 [25]. Liu et al. explored a novel auxetic lattice structure for femoral stems. FE analysis indicated that femoral stems with this auxetic structure reduced stress shielding more effectively than solid stems, particularly in the lateral zone [26]. Recent finite element studies have also compared the impact of material selection on bone remodeling. For instance, Ceddia et al. analyzed modular femoral stems with distal parts made from either Ti-6Al-4V or carbon fiber-reinforced polymer composites (CFRPCs) [27,28]. The results indicated that CFRPCs, due to their stiffness similarity with bone, promoted a more physiological stress distribution along the femur, supporting clinical observations of enhanced osseointegration and reduced proximal stress shielding.

In addition to geometric and lattice design approaches, biomimetic materials have been investigated to help reduce stress shielding. Bougherara et al. developed a biomimetic composite hip prosthesis featuring a polymer composite core coated with hydroxyapatite,

designed to mimic the mechanical properties of cortical bone [29]. Their findings showed that femoral bone implanted with this composite prosthesis could bear up to 192% more load than bone implanted with a conventional titanium (Ti) stem. This result indicates a substantial improvement in load distribution, with promising potential for reducing stress shielding. In another study, Ceddia et al. compared titanium and PEEK for spinal fixation via FE analysis [17]. The results showed that PEEK components resulted in significantly lower stress shielding and more favorable load transfer than titanium, highlighting its biomechanical compatibility and potential benefits in long-term fixation.

Biomimetic composites hold promise for implant applications due to their high biocompatibility and favorable balance of strength and stiffness.

Poly(lactic acid) (PLA) is a commonly used biocompatible polymer that is FDA-approved for clinical uses like surgical sutures and bone fixation. Its degradation pathway within the body is safe and supports the healing process. PLA's physical and mechanical properties can be adjusted through synthesis methods, stereoisomers, and molecular weight. For example, lower molecular weight PLA degrades more quickly, making it ideal for bone-healing applications. On the other hand, higher molecular weight PLA, although mechanically stronger, degrades more slowly and may induce inflammation, limiting its use in load-bearing implants [30–32]. To overcome the limitations of PLA in load-bearing applications, Gonzalez et al. developed a PLA-based composite by combining 3D-printed PLA layers with carbon fiber-reinforced composites (PLA/CFRCs). This composite exhibited promising thermal properties and substantial mechanical strength, with a tensile modulus of 19.29 ± 0.48 GPa and tensile strength of 238.91 ± 25.95 MPa. These properties are close to the mechanical range of human bone, making the composite suitable for use in prosthetic applications [33]. Similarly, Cheng et al. studied the mechanical performance of 3D-printed honeycomb composites reinforced with continuous fibers. These reinforced honeycomb structures were able to endure high amounts of deformation without catastrophic failure and displayed a shape-memory effect, recovering 87% of their original shape when heated. The inclusion of continuous fibers significantly enhanced the composite's properties, with specific energy absorption and specific stiffness values roughly double those of traditional honeycomb structures. These improvements make reinforced honeycombs ideal for applications in energy absorption, protective systems, and biomedical devices, where both strength and shape recovery are beneficial [34].

According to a review study conducted by Milazzo et al., another promising approach to improving PLA's functionality in implants involves reinforcing it with hydroxyapatite (HA) [35]. In HA-reinforced poly(lactic-co-glycolic acid) (PLGA) scaffolds, researchers achieved a modulus of elasticity (E) of 1.9 GPa and a compressive strength (CS) of 30 MPa, placing these properties between those of cancellous bone and cortical bone.

Poly(ether-ether-ketone) (PEEK) is a high-performance thermoplastic with unique properties that make it suitable for orthopaedic implants. Its excellent biological, mechanical, and chemical stability positions it as an ideal material for *in vivo* biomedical applications [36]. PEEK's mechanical properties closely resemble those of human bone, helping to reduce the likelihood of bone resorption and osteolysis associated with stress shielding in implants.

To assess the potential for reducing stress shielding, this study used finite element (FE) simulations to compare the mechanical behavior of an uncemented total hip arthroplasty (THA) model with PLA-HA and PEEK composite implants, incorporating two different stem lengths. Both implant models were tested in a synthetic bone model (Sawbone) to replicate real-world walking conditions. The hypothesis is that composite implants will demonstrate a lower stress shielding effect and less bone resorption compared with

traditional titanium implants, potentially improving long-term stability and integration with the body.

2. Materials and Methods

2.1. Geometry and Virtual Implant

The geometry employed for this study was the standardized femur model (mod. #3103), a recognized 3D surface model widely used in orthopaedic biomechanics [37].

NX v.2312 computer-aided design (CAD) software (Siemens) was utilized to create a model design based on a generic TriLock (DePuy) prosthesis (Figure 1).

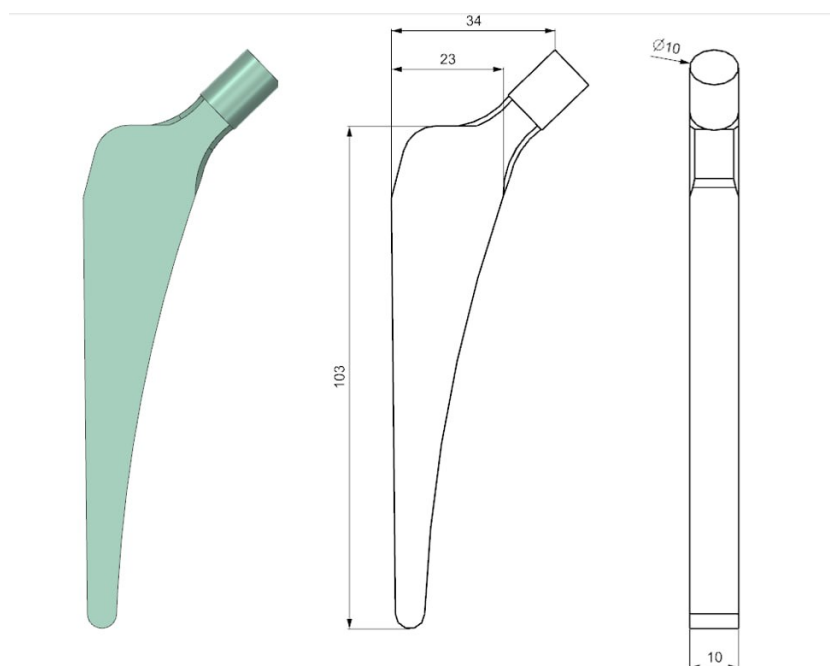


Figure 1. Implant geometry and main dimensions expressed in mm.

The stem dimensions were customized to achieve contact with the cortical bone without requiring any removal, optimizing primary stability.

In line with clinical practice, the femoral head was removed via a neck cut, and the implant was manually positioned such that the shaft axes of the femur and implant were nearly parallel. A Boolean operation was used to create a non-manifold assembly, simulating a cementless press fit.

2.2. Finite Element Model

The mesh for the bone-stem finite element model was generated using 4-noded tetrahedral elements (SOLID185 in ANSYS v2023 R1), which are suitable for capturing complex geometries and providing accurate stress distributions. A convergence study was conducted to determine an optimal element size, balancing computational cost and solution accuracy. The maximum element size was set to 3 mm. All materials were modeled as linear elastic and homogeneous isotropic, with the properties for the titanium, PLA reinforced with HA, and PEEK detailed in Table 1 [35,37,38].

To simulate full integration of the implant and analyze the stress around it, a bonded contact approach was applied, representing complete osseointegration at the implant–bone interface.

Table 1. Material properties.

Material	E [MPa]	ν
Cortical bone	18,600	0.3
Trabecular Bone	179	0.3
Titanium	118,000	0.33
PLA + HA	1900	0.3
PEEK	3000	0.38

2.2.1. Applied Loads and Boundary Conditions

The model's distal portion was fixed in place, simulating the stability provided by the surrounding skeletal structure. To replicate physiological loading during walking, a load was applied to the implant's head, reflecting a simulated 10-s walking cycle. For the intact bone, the same force was applied at the center of the femoral head and distributed across a group of neighboring surface nodes. Load values were calculated using Adams by inputting parameters such as the height and weight of a hypothetical subject, with the forces adjusted based on the provided femur length. These parameters were derived using formulas that account for body dimensions and femoral geometry [39,40] (Figure 2).

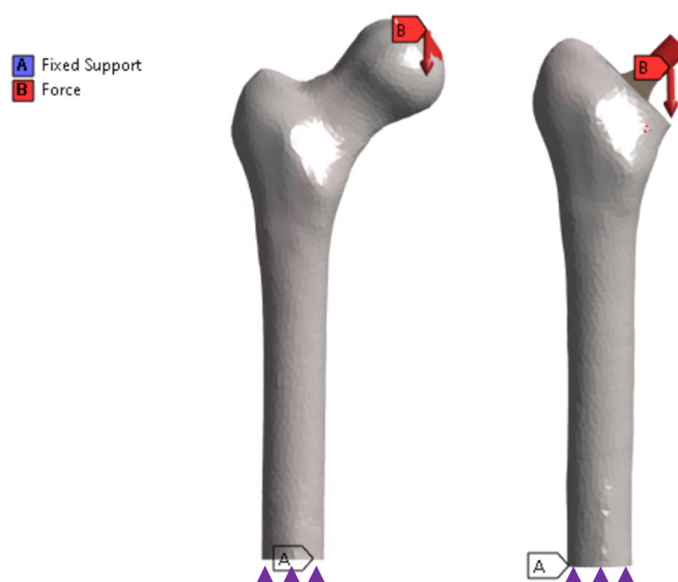


Figure 2. Boundary conditions (purple triangles) and loading set-up (red arrow) applied to the femur-implant system. The distal end of the femur was fully loaded while a load was applied on the femoral head to reproduce a single-leg stance condition during walking.

2.2.2. Bipedal Gait Cycle Load Calculus

The musculoskeletal and nervous systems are fundamental for human walking. During movement, the forces generated by the lower limbs are transmitted through joints, ligaments, and muscles to the trunk, while the inertial forces created by the movement of the upper limbs and the trunk help maintain balance, cooperating with those produced by the legs to achieve the necessary stability, as reported in [39]. Walking was chosen as the base movement for prosthesis optimization because it is an essential daily activity. In this work, an algorithm was designed to optimize a hip prosthesis through five stages: motion capture, joint angle extraction, creation of a human model, finite element analysis of the prosthesis, and result optimization using the gradient descent method. The model adopted in this paper was divided into sections for the upper limbs, trunk, and lower limbs, with 32 physical dimensions derived from anthropometric data [39,41,42]. The virtual model created in Adams uses the collected angular data to simulate movements. To simulate the

walking cycle, rotations were set at the joints responsible for movement (Figure 3). Finally, the reaction forces at the hip were calculated based on the forces exchanged between the feet and the ground. By tracing these forces up through the kinematic chain, the constraint reactions at the hip joint were defined. These forces will represent the loads exchanged with the hip prosthesis in question.

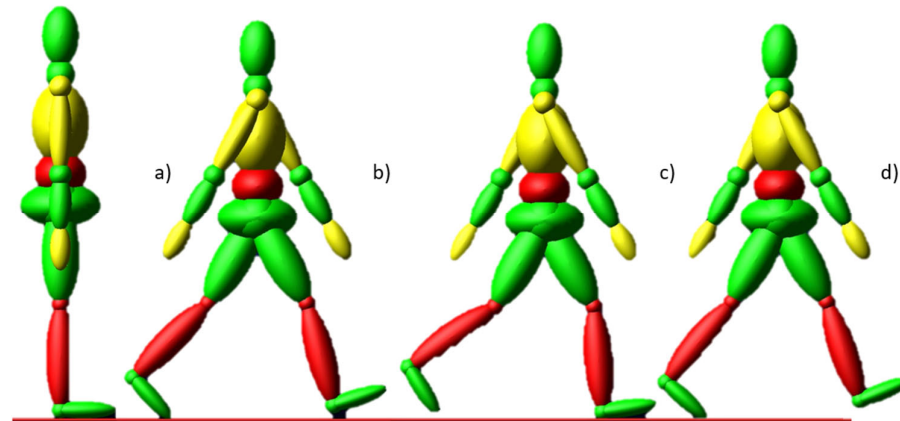


Figure 3. Bipedal gait cycle simulated by the virtual multibody model in Adams. It represents the sequence of motions involved in human walking: (a) heel strike, (b) stance, (c) toe-off, and (d) swing phases.

2.2.3. Measurements

According to Huiskes et al., strain energy density (SED) serves as an indicator of the bone remodeling stimulus [43]. Therefore, the SED was obtained and compared across each predefined Gruen zone ($i = 1-7$) [44] in both the intact and implanted models, with stress shielding quantified as follows:

$$SS(\%) = \frac{SED_{GruenZone^i}^{Intact} - SED_{GruenZone^i}^{Implant}}{SED_{GruenZone^i}^{Intact}}$$

A positive stress shielding (SS) indicates that the local region is under less stress than it was pre-surgery, potentially leading to stress shielding. Conversely, a negative SS suggests an increase in local stress or possible stress concentration [45]. SED strain measurements were acquired.

3. Results

Strain energy density (SED) was measured (Figure 4) in both the cancellous bone and prosthesis Gruen zone (GZ) regions under pre-operative and post total hip arthroplasty (THA) conditions (see Table 1). High Stress Shielding Index (SS) values indicate a significant reduction in equivalent stress in the femur after surgery, which may lead to bone loss due to an underloading effect. Conversely, a negative SS indicates that the region experienced increased stress compared with the pre-surgical state, suggesting reduced stress shielding. Ideally, the goal was to bring the SSI values close to zero, indicating no stress shielding and a more physiological load distribution across the bone.

In GZ1, the negative SS values for PEEK and PLA suggest that these materials increased stress in this region, promoting a more physiological load distribution than titanium. Titanium's slightly negative SS also reflects reduced stress shielding, though to a lesser extent than the composites.

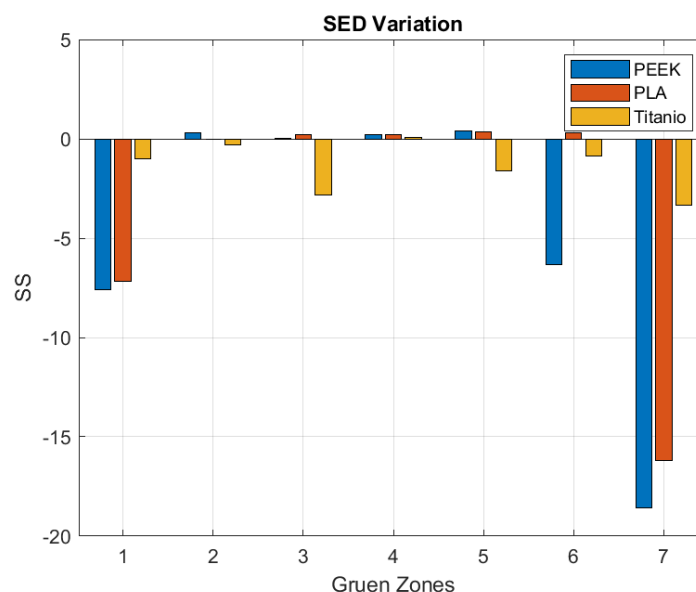


Figure 4. Stress shielding increase among the 7 Gruen zones. PEEK and PLA may offer a more physiological stress distribution, particularly in Gruen zones 1 and 7, where stress shielding (SS) reached its most negative values.

The SS values in GZ2–5 for all materials were close to zero, indicating minimal deviation from the natural stress distribution found in an intact femur. This suggests balanced load transfer for all implants in these regions, with little risk of stress shielding or stress concentration.

IN GZ6, PEEK, and to a lesser extent PLA, showed a more negative SS value, indicating that these implants increased stress in this distal region. Titanium’s SS in this zone remained nearly zero, indicating it maintained a stress distribution close to the intact bone’s load-bearing pattern without significant stress shielding or concentration.

GZ7 is the zone where PEEK and PLA exhibited markedly negative SS values, suggesting that these materials may load the distal femur region more effectively, reducing the likelihood of stress shielding and potentially supporting bone preservation. Titanium showed a smaller negative SS value, indicating less load transfer than PEEK and PLA but still a reduced level of stress shielding.

These findings are generally consistent with the literature data, which reported that the PEEK stem demonstrated minimal to no stress shielding in zones 2–5 and a substantially lower SSI than the titanium stem overall. These findings align with the previous literature, which suggests that reducing the elastic modulus of the implant material—bringing it closer to that of bone—can significantly mitigate stress shielding effects [46,47].

Figure 5 shows the von Mises stress distribution across femoral implants made from different materials, highlighting how stress varies from the neck to the distal tip. Figure 5a displays the titanium implant, where stress was highest at the proximal region (neck) and gradually decreased along the femur towards the distal tip. Figure 5b shows the PEEK implant, which exhibited a slightly lower maximum stress and a visibly smoother stress gradient across the femur, indicating a more even load distribution. Figure 5c illustrates the PLA implant, which presented the lowest peak stress among the three and a similar distribution pattern to PEEK, with an even lower stress concentration proximally.

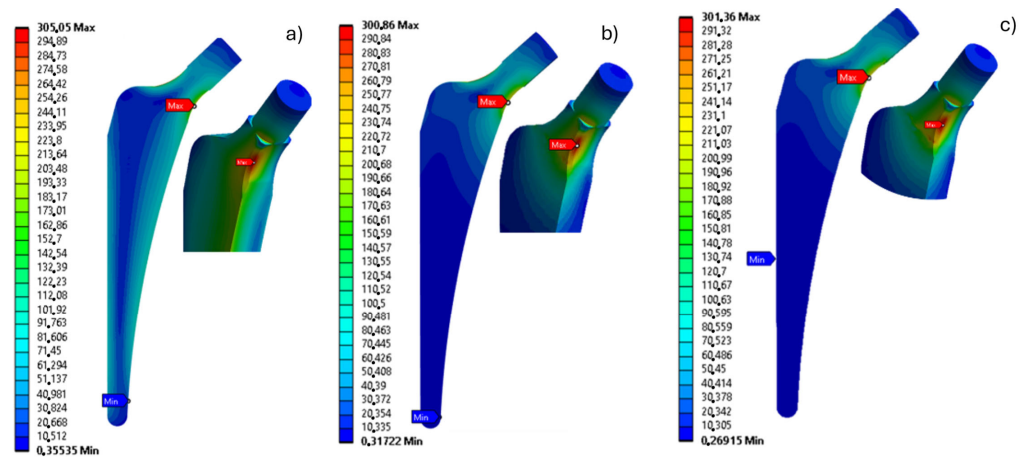


Figure 5. Comparison between (a) titanium, (b) PEEK, and (c) PLA implants, with von Mises stress distribution presented in section and three-dimensional views. The PLA implant registered the lowest stress concentration at the neck, showing the smoothest gradient of the three materials from the proximal to distal parts.

Although the reduction in peak stress between the materials may appear minor, a more in-depth quantitative analysis revealed substantial differences in how stress is distributed across the bone–implant interface. This was confirmed by a nodal stress evaluation, where the number of nodes exceeding a conservative threshold of 40 MPa—commonly associated with the onset of microdamage—was calculated [48]. The results show that a greater percentage of nodes experienced physiologically relevant stress levels in the PEEK (8.93%) and PLA (9.24%) cases, compared with only 5.98% in the titanium configuration, indicating a more effective load transfer to the surrounding bone in the less stiff materials.

This broader stress engagement implies that PEEK and PLA facilitate better load transfer to the surrounding bone, potentially minimizing stress shielding effects.

Additionally, a boxplot analysis (Figure 6) of nodal stress distributions supports this trend, showing that PEEK and PLA exhibited higher median stress values and a more uniform stress spread compared with titanium, which tends to concentrate stress more proximally.

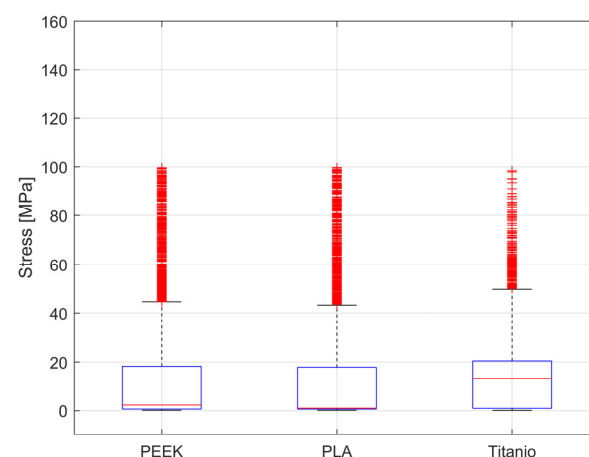


Figure 6. Boxplot of von Mises stress for each material. PLA and PEEK showed a distribution slightly shifted toward higher values compared with titanium, with a larger number of nodes exceeding 40 MPa (red crosses), indicating broader stress transfer in the surrounding bone.

These findings align with prior biomechanical theories, which suggest that reducing implant stiffness leads to more natural load-sharing but may increase stress at the interface, an effect observed here in the greater bone surface involvement for PEEK and PLA [49].

4. Discussion

Stress shielding has long been a challenge in total hip arthroplasty (THA), where conventional materials like titanium are prone to transferring limited load to surrounding bone tissue due to their high stiffness. This often leads to bone remodeling or resorption in underloaded regions, contributing to long-term complications such as implant loosening and osteolysis. While advantageous in terms of corrosion resistance and biocompatibility, this presents a modulus mismatch with bone that can result in bone deterioration over time. Previous studies have attempted to address this issue by incorporating lattice structures into titanium implants or exploring alternative materials that better mimic bone's mechanical properties. This study computationally evaluated the potential of PEEK and PLA composites to reduce stress shielding in femoral implants compared with traditional titanium, with the broader goal of extending implant lifespans and reducing failure rates associated with stress shielding. The findings suggest that composite materials like PEEK and PLA may offer a more physiological stress distribution, which could ultimately help mitigate bone resorption and enhance implant longevity.

This result suggests that these composites might distribute forces more effectively in load-bearing regions, potentially reducing bone resorption. Notably, PEEK, with a modulus closer to that of cortical bone, demonstrated enhanced load transfer in areas traditionally prone to stress shielding, indicating its potential as a viable alternative to titanium. While the peak stress reduction at the femoral neck was modest (approximately 1.5%), a more detailed nodal stress analysis provided a deeper insight; the percentage of nodes experiencing stress above a conservative fatigue threshold of 40 MPa was significantly higher for PEEK (8.93%) and PLA (9.24%) compared with titanium (5.98%). This indicates a broader and more physiologically relevant engagement of the bone-implant interface in the composite materials.

The observed improvements in stress distribution with PEEK and PLA composites have notable implications for the design of next-generation femoral implants. By more closely matching the mechanical properties of bone, these materials may improve implant fixation and minimize bone loss, thereby addressing a primary cause of implant failure: stress shielding. Additionally, the bioresorbable nature of PLA and the bioinert but modifiable properties of PEEK make them promising candidates for long-term applications where implant durability and biocompatibility are crucial.

Limitations and Future Perspectives

While this study presents promising insights into the use of PEEK and PLA composites in femoral implants, it presents several limitations. The femur model used in this study was based on a standardized 3D geometry rather than a CT scan from an individual requiring surgery. This generic model may not fully represent the complex anatomical variations found in patients with hip conditions or osteoporosis, potentially limiting the applicability of our findings to real-world scenarios. Future studies could address this by utilizing patient-specific CT data to better replicate the anatomy and the material properties of individuals likely to undergo THA.

The implant positioning in the model was manually adjusted *in silico*, rather than following a precise surgical technique or being subject to intraoperative constraints. As such, the alignment of the implant may not fully reflect the variability encountered in clinical practice. This could influence load transfer patterns, potentially affecting the simulation results. Incorporating more sophisticated positioning algorithms or simulating variations in implant placement could improve the clinical relevance of FE simulations.

Additionally, although the numerical results reflect realistic mechanical behavior, experimental validation remains essential. At present, we have compared our outcomes with

similar studies reported in the literature to verify their consistency. However, laboratory tests are planned as the next step to validate the simulation methodology and confirm its predictive reliability. Finally, this study evaluated implant performance under a single, simulated walking load. However, the femur is subjected to a wide range of loading conditions during daily activities, including climbing stairs, sitting down, and more dynamic forces associated with high-impact activities. Including multiple loading scenarios could provide a more comprehensive assessment of how these materials behave under different physiological conditions, enhancing the sensitivity and robustness of the FE model.

5. Conclusions

This study explored the potential of alternative biomaterials, specifically PEEK and PLA composites, for femoral implants in total hip arthroplasty (THA), assessing their ability to reduce stress shielding compared to traditional titanium implants. Finite element (FE) analysis revealed that both PEEK and PLA demonstrated promising load distribution patterns, with a tendency to better preserve stress levels across the bone, particularly in distal zones like Gruen zones 6 and 7. This suggests that these materials could help mitigate bone resorption and support long-term implant stability by providing a more physiological load transfer. In conclusion, PEEK and PLA composites represent promising materials for THA femoral stems, offering potential advantages over titanium in terms of reducing stress shielding and promoting bone preservation. Further studies that incorporate patient-specific geometries, heterogeneous bone properties, and a variety of loading scenarios are recommended to confirm these findings and guide the development of more effective, patient-centred implant solutions.

Author Contributions: Conceptualization, D.M. and M.S.; methodology, D.M.; software, D.M. and M.S.; validation, D.M. and M.S.; formal analysis, D.M.; investigation, D.M. and M.S.; resources, D.M.; data curation, M.S.; writing—original draft preparation, D.M. and M.S.; writing—review and editing, D.M.; visualization, D.M. and M.S.; supervision, D.M.; project administration, D.M. All authors have read and agreed to the published version of the manuscript.

Funding: This research received no external funding.

Institutional Review Board Statement: Not applicable.

Informed Consent Statement: Not applicable.

Data Availability Statement: The data presented in this study are available on request from the corresponding author.

Conflicts of Interest: The authors declare no conflict of interest.

References

1. International Osteoporosis Foundation | IOF. Available online: <https://www.osteoporosis.foundation/> (accessed on 15 November 2024).
2. Learmonth, I.D.; Young, C.; Rorabeck, C. The Operation of the Century: Total Hip Replacement. *Lancet* **2007**, *370*, 1508–1519. [[CrossRef](#)] [[PubMed](#)]
3. Joshi, M.G.; Advani, S.G.; Miller, F.; Santare, M.H. Analysis of a Femoral Hip Prosthesis Designed to Reduce Stress Shielding. *J. Biomech.* **2000**, *33*, 1655–1662. [[CrossRef](#)] [[PubMed](#)]
4. D’Andrea, D.; Risitano, G.; Desiderio, E.; Quintarelli, A.; Milone, D.; Alberti, F. Artificial Neural Network Prediction of the Optimal Setup Parameters of a Seven Degrees of Freedom Mathematical Model of a Race Car: IndyCar Case Study. *Vehicles* **2021**, *3*, 300–329. [[CrossRef](#)]
5. McCarthy, C.; Steinberg, G.; Agren, M.; Leahey, D.; Wyman, E.; Baran, D. Quantifying Bone Loss from the Proximal Femur after Total Hip Arthroplasty. *J. Bone Joint Surg. Br.* **1991**, *73-B*, 774–778. [[CrossRef](#)]
6. Viceconti, M.; Pancanti, A.; Varini, E.; Traina, F.; Cristofolini, L. On the Biomechanical Stability of Cementless Straight Conical Hip Stems. *Proc. Inst. Mech. Eng. H.* **2006**, *220*, 473–480. [[CrossRef](#)]

7. Sunavala-Dossabhoy, G.; Saba, B.M.; McCarthy, K. Strategic Debulking of the Femoral Stem Promotes Load Sharing Through Controlled Flexural Rigidity of the Implant Wall: Optimization of Design by Finite Element Analysis. *bioRxiv* **2024**. [\[CrossRef\]](#)
8. Dopico-González, C.; New, A.M.; Browne, M. Probabilistic Finite Element Analysis of the Uncemented Hip Replacement—Effect of Femur Characteristics and Implant Design Geometry. *J. Biomech.* **2010**, *43*, 512–520. [\[CrossRef\]](#)
9. Sumner, D.R. Long-Term Implant Fixation and Stress-Shielding in Total Hip Replacement. *J. Biomech.* **2015**, *48*, 797–800. [\[CrossRef\]](#)
10. Milošev, I.; Levašič, V.; Kovač, S.; Sillat, T.; Virtanen, S.; Tiainen, V.-M.; Trebše, R. Metals for Joint Replacement. In *Joint Replacement Technology*; Elsevier: Amsterdam, The Netherlands, 2021; pp. 65–122.
11. Uniyal, P.; Kumar, N.; Spataro, M. Microstructural and Dynamic Mechanical Behavior of the Cortical Bone. In *Dynamic Mechanical and Creep-Recovery Behavior of Polymer-Based Composites*; Elsevier: Amsterdam, The Netherlands, 2024; pp. 351–380.
12. Hanada, S.; Masahashi, N.; Jung, T.-K.; Yamada, N.; Yamako, G.; Itoi, E. Fabrication of a High-Performance Hip Prosthetic Stem Using β Ti–33.6Nb–4Sn. *J. Mech. Behav. Biomed. Mater.* **2014**, *30*, 140–149. [\[CrossRef\]](#)
13. Taylor, M.; Prendergast, P.J. Four Decades of Finite Element Analysis of Orthopaedic Devices: Where Are We Now and What Are the Opportunities? *J. Biomech.* **2015**, *48*, 767–778. [\[CrossRef\]](#)
14. Salunke, P.; Karthigeyan, M.; Uniyal, P.; Mishra, K.; Gupta, T.; Kumar, N. A Novel Pedicle Screw Design with Variable Thread Geometry: Biomechanical Cadaveric Study with Finite Element Analysis. *World Neurosurg.* **2023**, *172*, e144–e150. [\[CrossRef\]](#) [\[PubMed\]](#)
15. Sas, A.; Pellikaan, P.; Kolk, S.; Marty, P.; Scheerlinck, T.; van Lenthe, G.H. Effect of Anatomical Variability on Stress-shielding Induced by Short Calcar-guided Stems: Automated Finite Element Analysis of 90 Femora. *J. Orthop. Res.* **2019**, *37*, 681–688. [\[CrossRef\]](#) [\[PubMed\]](#)
16. Ceddia, M.; Romasco, T.; Comuzzi, L.; Specchiulli, A.; Piattelli, A.; Lamberti, L.; Di Pietro, N.; Trentadue, B. Finite-Element Analysis Study Comparing Titanium and Polyetheretherketone Caps in a Conometric Connection between Implant and Prosthesis. *Adv. Eng. Mater.* **2024**, *26*, 2400198. [\[CrossRef\]](#)
17. Ceddia, M.; Lamberti, L.; Trentadue, B. A Finite Element Study of Simulated Fusion in an L4-L5 Model: Influence of the Combination of Materials in the Screw-and-Rod Fixation System on Reproducing Natural Bone Behavior. *Biomimetics* **2025**, *10*, 72. [\[CrossRef\]](#)
18. Ceddia, M.; Solarino, G.; Tucci, M.; Lamberti, L.; Trentadue, B. Stress Analysis of Tibial Bone Using Three Different Materials for Bone Fixation Plates. *J. Compos. Sci.* **2024**, *8*, 334. [\[CrossRef\]](#)
19. Milone, D.; Nicita, F.; Cervino, G.; Santonocito, D.; Risitano, G. Finite Element Analysis of OT Bridge Fixed Prosthesis System. *Proc. Procedia Struct. Integr.* **2021**, *33*, 734–747. [\[CrossRef\]](#)
20. Al-Mukhtar, A.M. Fracture Mechanics and Micro Crack Detection in Bone: A Short Communication. In Proceedings of the Conference Medical Device Materials V. Novelty: ASM International, Minneapolis, MN, USA, 8–10 August 2011.
21. van den Munckhof, S.; Zadpoor, A.A. How Accurately Can We Predict the Fracture Load of the Proximal Femur Using Finite Element Models? *Clin. Biomech.* **2014**, *29*, 373–380. [\[CrossRef\]](#)
22. van Rietbergen, B.; Ito, K. A Survey of Micro-Finite Element Analysis for Clinical Assessment of Bone Strength: The First Decade. *J. Biomech.* **2015**, *48*, 832–841. [\[CrossRef\]](#)
23. Schileo, E.; Taddei, F.; Cristofolini, L.; Viceconti, M. Subject-Specific Finite Element Models Implementing a Maximum Principal Strain Criterion Are Able to Estimate Failure Risk and Fracture Location on Human Femurs Tested in Vitro. *J. Biomech.* **2008**, *41*, 356–367. [\[CrossRef\]](#)
24. Arabnejad, S.; Johnston, B.; Tanzer, M.; Pasini, D. Fully Porous 3D Printed Titanium Femoral Stem to Reduce Stress-Shielding Following Total Hip Arthroplasty. *J. Orthop. Res.* **2017**, *35*, 1774–1783. [\[CrossRef\]](#)
25. Cortis, G.; Mileti, I.; Nalli, F.; Palermo, E.; Cortese, L. Additive Manufacturing Structural Redesign of Hip Prostheses for Stress-Shielding Reduction and Improved Functionality and Safety. *Mech. Mater.* **2022**, *165*, 104173. [\[CrossRef\]](#)
26. Liu, B.; Wang, H.; Zhang, M.; Li, J.; Zhang, N.; Luan, Y.; Fang, C.; Cheng, C.-K. Capability of Auxetic Femoral Stems to Reduce Stress Shielding after Total Hip Arthroplasty. *J. Orthop. Translat* **2023**, *38*, 220–228. [\[CrossRef\]](#) [\[PubMed\]](#)
27. Ceddia, M.; Solarino, G.; Giannini, G.; De Giosa, G.; Tucci, M.; Trentadue, B. A Finite Element Analysis Study of Influence of Femoral Stem Material in Stress Shielding in a Model of Uncemented Total Hip Arthroplasty: Ti-6Al-4V versus Carbon Fibre-Reinforced PEEK Composite. *J. Compos. Sci.* **2024**, *8*, 254. [\[CrossRef\]](#)
28. Ceddia, M.; Trentadue, B.; Ceddia, M.; Trentadue, B. A Review of Carbon Fiber-Reinforced Polymer Composite Used to Solve Stress Shielding in Total Hip Replacement. *AIMS Mater. Sci.* **2024**, *11*, 449–462. [\[CrossRef\]](#)
29. Bougherara, H.; Bureau, M.; Campbell, M.; Vadean, A.; Yahia, L. Design of a Biomimetic Polymer-composite Hip Prosthesis. *J. Biomed. Mater. Res. A* **2007**, *82A*, 27–40. [\[CrossRef\]](#)
30. Marei, N.H.; El-Sherbiny, I.M.; Lotfy, A.; El-Badawy, A.; El-Badri, N. Mesenchymal Stem Cells Growth and Proliferation Enhancement Using PLA vs PCL Based Nanofibrous Scaffolds. *Int. J. Biol. Macromol.* **2016**, *93*, 9–19. [\[CrossRef\]](#)
31. Farah, S.; Anderson, D.G.; Langer, R. Physical and Mechanical Properties of PLA, and Their Functions in Widespread Applications—A Comprehensive Review. *Adv. Drug Deliv. Rev.* **2016**, *107*, 367–392. [\[CrossRef\]](#)

32. D'Andrea, D.; Milone, D.; Nicita, F.; Risitano, G.; Santonocito, D. Qualitative and Quantitative Evaluation of Different Types of Orthodontic Brackets and Archwires by Optical Microscopy and X-Ray Fluorescence Spectroscopy. *Prosthesis* **2021**, *3*, 342–360. [\[CrossRef\]](#)
33. Paz-González, J.A.; Velasco-Santos, C.; Villarreal-Gómez, L.J.; Alcudia-Zacarias, E.; Olivas-Sarabia, A.; Cota-Leal, M.A.; Flores-López, L.Z.; Gochi-Ponce, Y. Structural Composite Based on 3D Printing Polylactic Acid/Carbon Fiber Laminates (PLA/CFRC) as an Alternative Material for Femoral Stem Prosthesis. *J. Mech. Behav. Biomed. Mater.* **2023**, *138*, 105632. [\[CrossRef\]](#)
34. Cheng, Y.; Li, J.; Qian, X.; Rudykh, S. 3D Printed Recoverable Honeycomb Composites Reinforced by Continuous Carbon Fibers. *Compos. Struct.* **2021**, *268*, 113974. [\[CrossRef\]](#)
35. Milazzo, M.; Contessi Negrini, N.; Scialla, S.; Marelli, B.; Farè, S.; Danti, S.; Buehler, M.J. Additive Manufacturing Approaches for Hydroxyapatite-Reinforced Composites. *Adv. Funct. Mater.* **2019**, *29*, 1903055. [\[CrossRef\]](#)
36. Zhao, Y.; Wong, H.M.; Wang, W.; Li, P.; Xu, Z.; Chong, E.Y.W.; Yan, C.H.; Yeung, K.W.K.; Chu, P.K. Cytocompatibility, Osseointegration, and Bioactivity of Three-Dimensional Porous and Nanostructured Network on Polyetheretherketone. *Biomaterials* **2013**, *34*, 9264–9277. [\[CrossRef\]](#) [\[PubMed\]](#)
37. Viceconti, M.; Casali, M.; Massari, B.; Cristofolini, L.; Bassini, S.; Toni, A. The 'Standardized Femur Program' Proposal for a Reference Geometry to Be Used for the Creation of Finite Element Models of the Femur. *J. Biomech.* **1996**, *29*, 1241. [\[CrossRef\]](#) [\[PubMed\]](#)
38. Rae, P.J.; Brown, E.N.; Orler, E.B. The Mechanical Properties of Poly(Ether-Ether-Ketone) (PEEK) with Emphasis on the Large Compressive Strain Response. *Polymer* **2007**, *48*, 598–615. [\[CrossRef\]](#)
39. Milone, D.; D'Andrea, D.; Santonocito, D. Smart Design of Hip Replacement Prostheses Using Additive Manufacturing and Machine Learning Techniques. *Prosthesis* **2024**, *6*, 24–40. [\[CrossRef\]](#)
40. Crisafulli, D.; Spataro, M.; De Marchis, C.; Risitano, G.; Milone, D. A New Sensorized Approach Based on a DeepLabCut Model and IR Thermography for Characterizing the Thermal Profile in Knees During Exercise. *Sensors* **2024**, *24*, 7862. [\[CrossRef\]](#)
41. Milone, D.; Risitano, G.; Pistone, A.; Crisafulli, D.; Alberti, F. A New Approach for the Tribological and Mechanical Characterization of a Hip Prosthesis Through a Numerical Model Based on Artificial Intelligence Algorithms and Humanoid Multibody Model. *Lubricants* **2022**, *10*, 160. [\[CrossRef\]](#)
42. Milone, D.; Longo, F.; Merlino, G.; De Marchis, C.; Risitano, G.; D'Agati, L. MocapMe: DeepLabCut-Enhanced Neural Network for Enhanced Markerless Stability in Sit-to-Stand Motion Capture. *Sensors* **2024**, *24*, 3022. [\[CrossRef\]](#)
43. Huiskes, R.; Weinans, H.; Grootenboer, H.J.; Dalstra, M.; Fudala, B.; Slooff, T.J. Adaptive Bone-Remodeling Theory Applied to Prosthetic-Design Analysis. *J. Biomech.* **1987**, *20*, 1135–1150. [\[CrossRef\]](#)
44. Gruen, T.A.; McNeice, G.M.; Amstutz, H.C. "Modes of Failure" of Cemented Stem-Type Femoral Components. A Radiographic Analysis of Loosening. *Clin. Orthop. Relat. Res.* **1979**, *141*, 17–27.
45. Boyle, C.; Kim, I.Y. Comparison of Different Hip Prosthesis Shapes Considering Micro-Level Bone Remodeling and Stress-Shielding Criteria Using Three-Dimensional Design Space Topology Optimization. *J. Biomech.* **2011**, *44*, 1722–1728. [\[CrossRef\]](#) [\[PubMed\]](#)
46. Morscher, E.; Dick, W. Cement Less Fixation of Isoelastic Hipendoprotheses Manufactured from Plastic Materials. *Clin. Orthop. Relat. Res.* **1983**, *176*, 77–87.
47. Naghavi, S.A.; Lin, C.; Sun, C.; Tamaddon, M.; Basiouny, M.; Garcia-Souto, P.; Taylor, S.; Hua, J.; Li, D.; Wang, L.; et al. Stress Shielding and Bone Resorption of Press-Fit Polyether–Ether–Ketone (PEEK) Hip Prosthesis: A Sawbone Model Study. *Polymers* **2022**, *14*, 4600. [\[CrossRef\]](#) [\[PubMed\]](#)
48. Taylor, D. Fatigue of Bone and Bones: An Analysis Based on Stressed Volume. *J. Orthop. Res.* **1998**, *16*, 163–169. [\[CrossRef\]](#)
49. Huiskes, R.; Weinans, H.; van Rietbergen, B. The Relationship between Stress Shielding and Bone Resorption around Total Hip Stems and the Effects of Flexible Materials. *Clin. Orthop. Relat. Res.* **1992**, *274*, 124–134. [\[CrossRef\]](#)

Disclaimer/Publisher's Note: The statements, opinions and data contained in all publications are solely those of the individual author(s) and contributor(s) and not of MDPI and/or the editor(s). MDPI and/or the editor(s) disclaim responsibility for any injury to people or property resulting from any ideas, methods, instructions or products referred to in the content.